DALTON
FULL PAPER

Oxidative degradation of monomeric and dimeric phenylpropanoids: reactivity and mechanistic investigation

Carmen Canevali,*[a] Marco Orlandi,[b] Luca Pardi,[c] Bruno Rindone,[b] Roberto Scotti,[a] Jussi Sipila[d] and Franca Morazzoni[a]

[a] *Dipartimento di Scienza dei Materiali, Università di Milano-Bicocca, Via R. Cozzi 53, 20125 Milano, Italy. E-mail: Carmen.Canevali@mater.unimib.it*
[b] *Dipartimento di Scienze dell' Ambiente e del Territorio, Università di Milano-Bicocca, Piazza della Scienza 1, 20126 Milano, Italy*
[c] *Istituto per i Processi Chimico Fisici, Consiglio Nazionale delle Ricerche, Via G. Moruzzi 1, 56124 Pisa, Italy*
[d] *Laboratory of Organic Chemistry, University of Helsinki, P.O. Box 55, FIN-00014, Helsinki, Finland*

Received 5th April 2002, Accepted 27th May 2002
First published as an Advance Article on the web 2nd July 2002

The oxidative degradation of lignin related model compounds catalysed by [*N*,*N′*-bis(salicylidene)ethane-1,2-diaminato]cobalt(II), [Co(salen)], have been studied in chloroform. Arylglycerol β-aryl ethers, phenylcoumarans and apocynol showed very high conversion values within 30 minutes of the start of the reaction and their conversion rates were higher than those reported for phenylpropenoidic compounds, methyl (*E*)-ferulate and methyl (*E*)-4-hydroxycinnamate. The results of the CW electron paramagnetic resonance (EPR) investigation using the X-band, performed at the reaction temperature (298 K) showed that two phenoxy cobalt radicals ($[Co^{III}(salen)(ROH)(RO^{\bullet})]$ and $[Co^{III}(salen)(RO^{-})(RO^{\bullet})]$) are involved in the oxidation mechanism of all the phenol compounds ROH. In a frozen solution the $[Co^{III}(salen)(ROH))(RO^{\bullet})]$ radical prevailed and its axial magnetic anisotropy was determined using high frequency, 190 GHz, CW EPR spectra. The X-band EPR monitoring of the phenoxy cobalt radicals during the reaction showed a faster decrease in the amounts of radical in the oxidation of propanoidic phenols compared with that of propenoidic phenols. The lifetime of the radicals formed from substrates having a methoxy group *ortho* to the aromatic hydroxy was also shorter than from substrates lacking this functionality. Both reactivity and spectroscopic data suggest that the lifetime of the phenoxy cobalt radicals correlates with the conversion rates of the substrates.

Introduction

The use of renewable biomass as raw material for the production of chemicals is an important component of international energy policy. Due to its high abundance in the biosphere, one of the most interesting renewable but generally neglected carbon sources is lignin, which is present in the woody structure of higher plants, typically 30% of dry weight.[1] Lignin is a structurally highly intricate aromatic polymer of oxygenated phenylpropane units.[2–6] Several interunit carbon–carbon and carbon–oxygen bonds are present in its structure and the relative abundance of these interunit linkages varies for different types of wood. Many studies have focused on the oxidative degradation of lignin to give useful low molecular weight aromatic compounds. These processes are commercially important and may be performed by oxidation with nitroaromatics,[7] with air in alkaline solution,[8] with ozone[9] and by electrochemical means.[10] Also the biomimetic procedures that use "activated" oxygen, such as laccase-mediated processes[11] or those mediated by binuclear Mn complexes,[12] have been shown to be potentially available technologies for obtaining low molecular weight compounds. The most promising biomimetic degradation systems use dioxygen as the oxidant and cobalt complexes as catalysts. Drago *et al.* showed that dioxygen was able to oxidise, in very good yield, isoeugenol to vanillin, using [bis(salicylidene-γ-iminopropyl)methylamine]cobalt(II), [Co(SMDPT)], as catalyst;[13] Bozell *et al.* reported the oxidation of *para*-substituted phenolic compounds to benzoquinones using [*N*,*N′*-bis (salicylidene)ethane-1,2-diaminato]cobalt(II), [Co(salen)], as catalyst;[14,15] Haikarainen *et al.* reported the oxidation in aqueous solution of lignin model compounds using a water-soluble [Co(salen)] derivative, (*N*,*N′*-bis{3,5-bis[(triphenylphosphonium) methyl]salicylidene}ethane-1,2-diaminato)cobalt(II), as catalyst to obtain vanillin and biphenylic products.[16]

We have recently reported that simple model compounds for the polyphenols contained in the waste waters from the paper industry can be degraded by oxidation with dioxygen, using [Co(salen)] as catalyst.[17] The mechanism of the reaction was elucidated by studying the degradation of several propenoidic phenols with different electron donor properties and by monitoring the processes by electron paramagnetic resonance (EPR) spectroscopy.[18] However our investigation into the active species focused on the simplest model compounds for lignin, containing only one aromatic ring with extended double bond–ester conjugation[18] (compounds **1** and **2** in Scheme 1). Since very small amounts of such structures are present in lignin waste material, we also decided to test model compounds representing more abundant structural units in residual lignin[19] as substrates for oxidation (phenylpropanoidic compounds **3**–**8** in Schemes 2–4). The reactivity of each compound was calculated as a measure of the conversion rate (percentage disappearance of starting material) and the product distribution was determined after methylation, using gas liquid chromatography-mass spectrometry (GLC-MS).

In order to confirm our previously hypothesised mechanism

DOI: 10.1039/b203386k

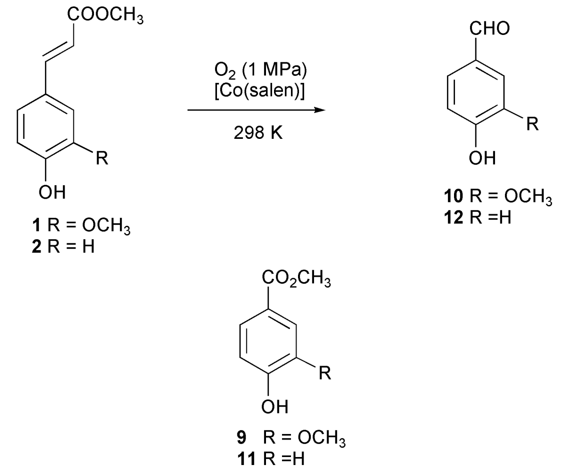

Scheme 1

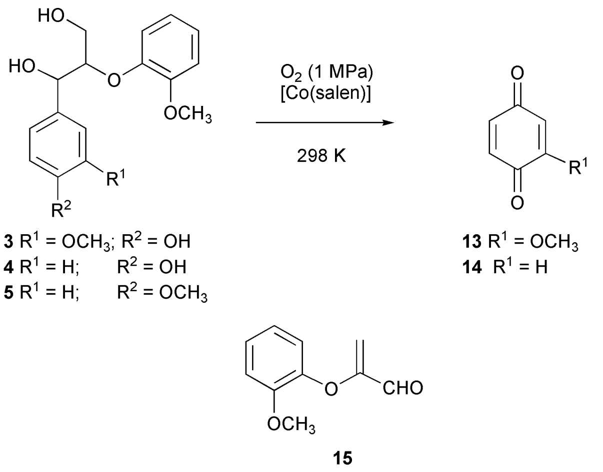

Scheme 2

for these types of reactions[18] and to give further insight into the molecular structure of the intermediate active radical compounds, we also identified the paramagnetic species active in the oxidation mechanism by EPR spectroscopy, both at the reaction temperature (298 K) in liquid samples and in frozen samples (200–10 K), combining the results of the X-band and 190 GHz spectra. The monitoring of paramagnetic species during the oxidation of phenylpropanoidic compounds, performed at the X-band frequency by cooling sample aliquots in liquid nitrogen to slow down the reaction, also allowed us to compare the reactivity of these model compounds with those of the phenylpropenoidic model compounds.

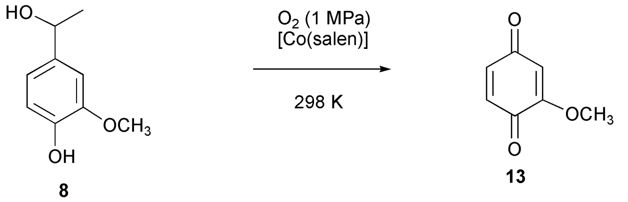

Scheme 4

Experimental

Reagents

The catalyst compound [Co(salen)] (99%) and the 1,4-benzoquinone were from Aldrich. Chloroform (Fluka) was used as received. Horseradish peroxidase (HRP) (E 1.11.1.7) was from Sigma, activity 429 U mg^{-1}.

1-(4-Hydroxy-3-methoxyphenyl)ethanol (apocynol) **8**, was prepared from acetovanillone (commercial grade Aldrich) as described by Bailey and Dence.[20]

The dimeric substrates 3-(4-hydroxy-3-methoxyphenyl)-2-(2-methoxyphenoxy)propane-1,3-diol **3**, 3-(4-hydroxyphenyl)-2-(2-methoxyphenoxy)propane-1,3-diol **4** and 3-(4-methoxyphenyl)-2-(2-methoxyphenoxy)propane-1,3-diol **5** were prepared according to the method of Sipila and Syrjanen.[21] Methyl (*E*)-[(2*RS*,3*SR*)-2,3-dihydro-2-(4-hydroxy-3-methoxyphenyl)-7-methoxy-3-methoxycarbonyl-1-benzofuran-5-yl]propenoate **6** was prepared according to the method of Orlandi *et al.*[22]

Methyl (*E*)-[(2*RS*,3*SR*)-2,3-dihydro-2-(4-hydroxyphenyl)-3-methoxycarbonyl-1-benzofuran-5-yl]propenoate **7** was synthesized as follows: methyl *p*-hydroxycinnamate **2** (2.80 g) was dissolved in dioxane (150 cm^3) and phosphate–citric acid buffer solution (pH 3.5, 0.002 M, 350 cm^3) was added. Aqueous hydrogen peroxide (1 M, 8.00 mmol) and HRP (1230 U) were added over 20 minutes. The mixture was stirred for 2.5 h at room temperature, then extracted with ethyl acetate (4 × 100 cm^3). The combined organic extracts were washed with 5% aqueous $NaHCO_3$ (40 cm^3), water (40 cm^3) and dried over Na_2SO_4. The solvent was evaporated under reduced pressure, and the residue was chromatographed on a silica gel flash column with hexane–ethyl acetate (gradient mode, from 4 : 1 to

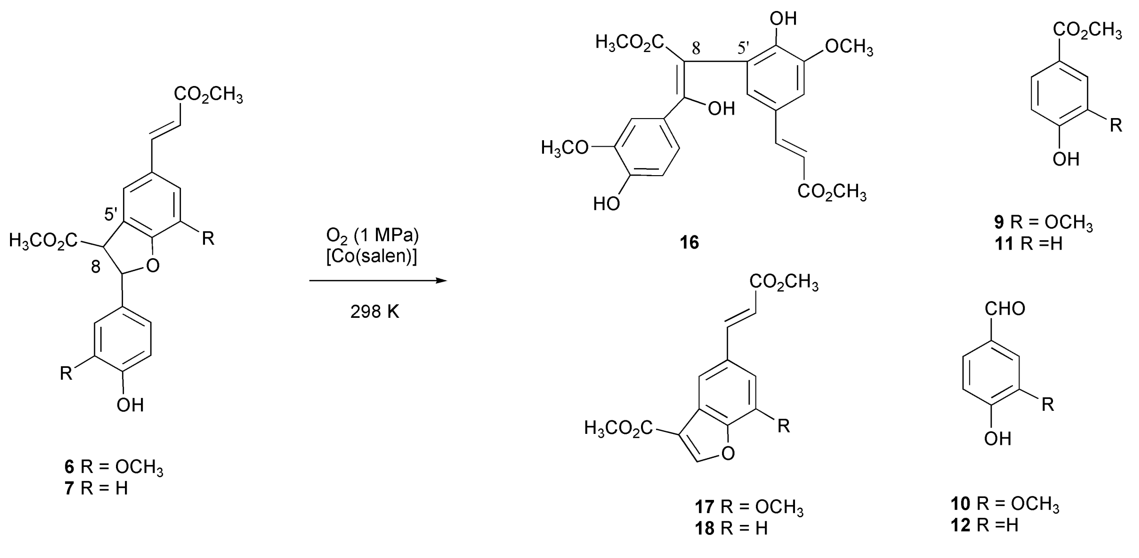

Scheme 3

1 : 1), yielding the phenyl-2,3-dihydrobenzofuran **7** (0.55 g, 50%); mp 82 °C (from methanol); ^{1}H NMR(CDCl$_3$): δ_H 7.63 (1 H, d, $J = 15.0$ Hz, 1 CH), 6.90–7.30 (7 H, m, 7 CH, aromatics), 6.31 (1 H, d, $J = 15.0$ Hz, 1 CH), 6.08 (1 H, d, $J = 8.0$ Hz, 1 CH), 5.50 (1 H, s, 1 OH), 4.33 (1 H, d, $J = 8.0$ Hz, 1 CH), 3.83 (3 H, s, 1 CH$_3$), 3.80 (3 H, s, 1 CH$_3$); MS (EI): m/z 354 (M$^+$) (100), 322 (98), 290 (60). Elemental analysis: C, 67.19; H, 5.12 (calculated for $C_{20}H_{18}O_6$); C, 67.68; H, 5.09 (experimental).

Apparatus and measurements

Melting points were determined with a Büchi MP 19 apparatus and are uncorrected. Mass spectra were performed using the direct injection system mode with positive electron impact on a VG 7070 EQ instrument.

IR spectra were recorded on a FTIR Perkin-Elmer 1725X spectrophotometer. ^{1}H and ^{13}C NMR spectra were recorded by a Bruker AC 300 or a Bruker AMX 300 instruments (in CDCl$_3$ solutions). Chemical shift values (δ) are given as ppm relative to the tetramethylsilane resonance and coupling constant values (J) are measured in Hz. HPLC analyses were performed using a combination of a Waters 600E pump, column (Kromasil C18, 250 × 4.6 mm, 5 µm) and HP 9153C photodiode array detector. The column was eluted using a flow rate of 1.0 cm^3 min^{-1} at room temperature with the following gradient: 0–2 min, CH$_3$CN–H$_2$O 60 : 40; 2–13 min, CH$_3$CN–H$_2$O 95 : 5; 13–15 min, CH$_3$CN–H$_2$O 60–40; 15–20 min, CH$_3$CN–H$_2$O 60 : 40. The GLC-MS analyses were performed using a HP 5890 gas chromatograph, interfaced with a quadrupole detector (HP 5970) operating in electron impact mode 70 eV. The gas chromatograph was equipped with a Supelco SPB-5 (95% dimethylpolisiloxan) capillary column (length 30 m, inner diameter 0.25 mm, film thickness 0.25 µm). The column was eluted at 333 K for 2 min, followed by a temperature gradient from 333 K to 523 K at 283 K min^{-1}. The carrier gas used was helium at a flow rate of 40 cm^3 s^{-1}.

The X-band CW EPR spectra were recorded on a Bruker EMX spectrometer. Temperature control in the range 4–300 K was achieved through an Oxford Instrument for X-band spectroscopy. The CW high frequency (HF) EPR spectra were recorded on a HF-EPR spectrometer that can operate at three frequencies: 95, 190 and 285 GHz. Fundamental monochromatic radiation in the range 94–96 GHz was delivered by a Gunn effect diode (RPG Instruments, Meckenheim, Germany) with an output power of 40 mW. The two upper harmonics were generated by non-linear solid state devices which work as a doubler and tripler. The frequency and phase of the source was stabilized by means of a phase lock loop system. The magnetic system was a superconductor magnet (Oxford Instruments Ltd.) that can be continuously swept to a maximum field of 12 T with a constant relative homogeneity of 10 ppm. The magnet system was equipped with a sweep coil that was used to sweep the field through the EPR line, keeping the main coil constant at a given field value. The maximum sweep range was ±0.2 T. An enhanced hot electrons bolometer (InSb) operating in liquid helium (QMC instruments Ltd, Billingshurst, UK) was used as the detector. The sample probe is an ultra-wide band probe similar to those used in other laboratories.[23] The system was not equipped with a resonating structure. The sample was placed in the volume of maximum homogeneity in an overmoded cylindrical metallic wave-guide mounted axially in the static magnetic field. The liquid sample was held in a 4 cm long Teflon bucket of 9 mm internal diameter. A modulation coil was mounted around the sample holder delivering an a.c. magnetic field of 0.2 mT maximum amplitude. Temperature control in the range 4–300 K was achieved through an Oxford Instrument system based on the use of a static continuous flow cryostat (CF1200, Oxford Instr.) and a PID temperature control method. The temperature stability was 0.01 K at liquid helium temperature.

Table 1 Conversion (%) at different reaction times for the oxidation in chloroform of the phenylpropenoidic compounds, the β-*O*-4 and β-5 type dimeric compounds, shown in Schemes 1–3

Compound	Conversion (%)			
	30 min	1 h	5 h	48 h
1[18]	60 ± 5	84 ± 6	88 ± 4	99 ± 1
2[18]	1 ± 0.5	6 ± 3	37 ± 4	60 ± 4
3	90 ± 6	98 ± 5	99 ± 1	99 ± 1
4	70 ± 5	83 ± 4	96 ± 3	98 ± 1
5	50 ± 10	66 ± 8	70 ± 7	98 ± 1
6	99 ± 1	99 ± 1	99 ± 1	99 ± 1
7	83 ± 4	86 ± 5	99 ± 1	99 ± 1

The paramagnetic species active in the oxidation mechanism were identified using solutions prepared as follows: [Co(salen)] (6 × 10^{-3} M) was added to a deaerated CHCl$_3$ solution of the substrate (6 × 10^{-2} M), then the solution was allowed to react with oxygen (1 MPa pressure) at 298 K. After 20 min, the solution was deaerated by repeated freeze–vacuum treatments, then the spectrum was recorded at the indicated temperature under an argon atmosphere, in order to avoid line broadening due to the interaction of the paramagnetic species with dioxygen. The spectra from 298 K to 10 K were recorded at 9.5 GHz microwave frequency, those from 200K to 10 K also at 190 GHz. The oxidation reactions were monitored by taking aliquots of the reaction solution at the following reaction times (expressed in minutes): 5, 10, 15, 20, 30, 45, 60, 120, 180, 210, 240, 270, 300, and by immediately cooling them in liquid nitrogen to slow down the reaction. The X-band EPR spectra were recorded at 123 K.

The g values were measured by standardisation with diphenylpicrylhydrazyl (DPPH). The amount of paramagnetic species were calculated by double integration of the resonance line areas. All the experimental spectra were fitted by the 6/9/91 DOS version of the SIM14S simulation program.

Oxidation reactions

A CHCl$_3$ solution (40 cm^3) of substrate (6 × 10^{-2}M) and [Co(salen)] (6 × 10^{-3} M) was placed in a glass vessel (100 cm^3) and inserted into an autoclave (250 cm^3). The autoclave was charged with dioxygen (1 MPa) and left at 298 K for the time specifically indicated in Tables 1–3. The solvent was then evaporated under reduced pressure at room temperature and the residue was resolved on a silica gel column with a gradient of ethyl acetate–hexane (3 : 7 to 7 : 3) as eluents.

The identification of benzoic acid derivatives **9** and **11** and benzaldehyde derivatives **10** and **12** (Scheme 1) has already been reported.[18] The quinones **13** and **14** (Scheme 2) were identified by comparison with authentic samples.[24] The conjugated methylenic aldehyde **15** (Scheme 2), the open ring product **16** (Scheme 3) and the benzofuran structures **17** and **18** were identified by mass spectrometry, ^{1}H-NMR, ^{13}C-NMR, IR and UV spectroscopies.

Compound **15**: MS (EI): $m/z = 178$ (M$^+$, 100%), 149 (38), 108 (60), 77 (50); ^{1}H-NMR (CDCl$_3$): δ_H 3.79 (3 H, s, 1 CH$_3$), 5.05 (1 H, d, $J = 2$ Hz, 1 CH), 5.25 (1 H, d, $J = 2$ Hz, 1 CH), 6.85–7.25 (4 H, m, 4 CH, aromatics), 9.45 (1 H, s, 1 CHO); ^{13}C-NMR (CDCl$_3$): δ_C 56.4 (CH$_3$), 110.1 (CH$_2$), 114.8 (CH), 118.3 (CH), 121.6 (CH), 123.7 (CH), 143.0 (C), 155.0 (C), 166.9 (C), 189.5 (CH); IR (Nujol): ν_{max}/cm^{-1} 1703 (C=C–CO), 1617 (C=C–Ar); mp = 160 °C (from methanol).

Compound **16** (isolated after methylation): MS (EI): m/z = 472 (M$^+$, 15%), 457 (25), 442 (50), 428 (60); ^{1}H-NMR (CDCl$_3$): δ_H 3.70 (3 H, s, 1 CH$_3$), 3.75 (3 H, s, 1 CH$_3$), 3.78 (3 H, s, 1 CH$_3$), 3.85 (3 H, s, 1 CH$_3$), 4.00 (3 H, s, 1 CH$_3$), 4.06 (3 H, s, 1 CH$_3$), 4.10 (3 H, s, 1 CH$_3$), 6.80–7.20 (5 H, m, 5 CH), 6.31 (1 H, d, $J =$ 16 Hz, 1 CH), 7.75 (1 H, d, J = 16Hz, 1 CH); ^{13}C-NMR

Table 2 Product distribution (%) after 48 h for the oxidation in chloroform of the phenylpropenoidic compounds, the β-*O*-4 and β-5 type dimeric compounds, shown in Schemes 1–3

	Product and product distribution (%) after 48 h					
Compound	Benzoic acid derivative	Benzaldehyde derivative	Quinone derivative	Conjugated aldehyde derivative	Benzofuran derivative	8–5′ Hydroxylated ferulate dimer
1[18]	**9** 61 ± 4	**10** 39 ± 3	—			
2[18]	**11** 1 ± 0.5	**12** 43 ± 4	—			
3	—	—	**13** 16 ± 2	**15** 81 ± 1		
4	—	Traces	**14** 3 ± 1	**15** 20 ± 1		
5	—	Traces	—	—		
6	**9** 10 ± 1	**10** 5 ± 1	—		**17** 15 ± 1	**16** 55 ± 2
7	**11** 10 ± 1	**12** 4 ± 2	—		**18** 20 ± 1	—

Table 3 X-Band EPR data which fit the spectra recorded at 298 K after 20 minutes of reaction on substrates reported in Schemes 1–4

Compound	g_{I}	A_{I}/G	ΔH_{I}/G	g_{II}	A_{II}/G	ΔH_{II}/G	I : II
1	1.999	10.0	2.6	2.000	11.2	3.6	1 : 1
2	1.999	9.0	2.9	1.999	9.8	3.1	1 : 1
3	1.998	10.2	5.9	1.999	10.8	4.6	2 : 1
4	1.998	8.8	4.1	1.999	9.6	3.8	2 : 1
6	1.999	10.1	2.9	1.999	10.9	3.6	1 : 1
7	1.998	8.9	4.2	1.999	9.8	3.5	2 : 1
8	1.998	10.1	6.1	1.999	10.9	3.2	2 : 1

($CDCl_3$): δ_C 51.8 (CH_3), 51.3 (CH_3), 52.3 (CH_3), 56.8 (CH_3), 56.8 (CH_3), 56.8 (CH_3), 56.8 (CH_3), 93.0 (CH), 112.8 (CH), 112.8 (CH), 115.8 (CH), 117.1 (CH), 119.3 (CH), 119.4 (CH), 121.4 (C), 127.8 (CH), 127.9 (C), 141.3 (C), 144.6 (CH), 146.8 (C), 146.9 (C), 148.3 (C), 158.9 (C), 166.3 (C), 166.4 (C); IR (Nujol): ν_{max}/cm^{-1} 1720 (C=C–CO), 1460 (OCH_3), 1149 (C=C–OCH_3); UV (CH_2Cl_2): λ_{max}/nm 228, 300, 400.

Compound **17**: MS (EI): *m*/*z* = 290 (M^+, 100%), 259 (25), 277 (60), 199 (12); ^{1}H-NMR ($CDCl_3$): δ_H 3.83 (3 H, s, 1 CH_3), 3.83 (3 H, s, 1 CH_3), 3.92 (3 H, s, 1 CH_3), 6.45 (1 H, d, J = 16 Hz, 1 CH), 7.75 (1 H, d, J = 16 Hz, 1 CH), 7.05 (1 H, s, 1 CH), 7.85 (1 H, s, 1 CH), 8.29 (1 H, s, 1 CH); ^{13}C-NMR ($CDCl_3$): δ_C 52.3 (CH_3), 52.3 (CH_3), 56.8 (CH_3), 115.8 (CH), 116.1 (C), 118.3 (CH), 118.4 (CH), 127.2 (C), 130.6 (C), 141.3 (C), 145.6 (CH), 148.3 (C), 154.4 (CH), 166.3 (C), 166.4 (C); IR (Nujol): ν_{max}/cm^{-1} 1724 (CO), 1461 (OCH_3); UV (CH_2Cl_2): λ_{max}/nm 230, 265, 289.

The benzofuran structure **18** was identified by the following spectroscopic data:

MS (EI): *m*/*z* = 260(M^+ 100%), 229 (35), 247 (80); ^{1}H-NMR ($CDCl_3$): δ_H 3.83 (3 H, s, 1 CH_3), 3.83 (3 H, s, 1 CH_3), 6.45 (1 H, d, J = 16Hz, 1 CH), 7.75 (1 H, d, J = 16Hz, 1 CH), 7.05 (1 H, s, 1CH), 7.85 (1 H, s, 1 CH), 7.90 (1 H, s, 1 CH), 8.29 (1 H, s, 1 CH); ^{13}C-NMR ($CDCl_3$): δ_C 52.3 (CH_3), 52.3 (CH_3), 115.8 (CH), 116.1 (C), 118.3 (CH), 118.4 (CH), 127.2 (C), 130.6 (C), 141.3 (C), 145.6 (CH), 148.3 (C), 154.4 (CH), 166.3 (C), 166.4 (C); IR (Nujol): ν_{max}/cm^{-1} 1724 (CO), 1461 (OCH_3); UV (CH_2Cl_2), λ_{max}/nm 230, 265, 289.

The conversion rate (measured as percentage disappearance of the starting material) at 30 min, 1 h, 5 h and 48 h was obtained by high performance liquid chromatography-diode array detector (HPLC-DAD) analysis, using calibration curves with biphenyl as the internal standard.

The product distribution was determined 48 h from the start of the reaction by dissolving the residue in a mixture of acetone (20 cm^3) and dimethyl sulfate (0.3 cm^3), and adding K_2CO_3 (0.435 g). After refluxing for 2 h, the solid was filtered out and the solvent evaporated under reduced pressure; the residue was dissolved in CH_2Cl_2 and analysed by gas liquid chromatography-mass spectrometry (GLC-MS) using biphenyl as the internal standard.

Results

Oxidation reactions

The results of the oxidation of **1** and **2** propenoidic phenols in chloroform (Scheme 1) have been previously reported.[17,18] Here we extend the study to more significant lignin-like materials, phenylpropanoidic compounds **3**–**5** (β-*O*-4 type compounds), **6** and **7** (β-5 type compounds) and **8** (apocynol) (Schemes 2–4).

The results concerning the conversion of arylglycerol β-aryl ethers **3** and **4** and phenylcoumarans † **6** and **7** are collected in Table 1. All these dimeric compounds showed high conversion values within 30 minutes of the start of the reaction; conversion rates were higher than for the monomeric phenylpropenoidic phenols **1** and **2**. The distribution of the main aromatic products 48 hours after the onset of oxidation of **3**, **4**, **6** and **7** in chloroform is reported in Table 2. No polymerisation products were observed and aliphatic low molecular weight compounds due to further aromatic ring oxidation were not investigated. Phenolic arylglycerol β-aryl ethers **3** and **4** gave quinones **13** and **14** and the conjugated aldehyde **15** as the main reaction products (Scheme 2). Aldehyde **15** has already been isolated from the same substrates treated with oxygen in alkaline media.[23] The oxidation of phenylcoumaran **6** gave four main aromatic compounds: **9**, **10**, **16** and **17** (Scheme 3). Compounds **9**, **10** and **17** are fragmentation products, while compound **16** is an oxidation product. The oxidation of phenylcoumaran **7**, in which the *ortho* methoxy group is absent, gave only three fragmentation products, **11**, **12** and **18** (Scheme 3).

The β-*O*-4 compound **5**, in which the phenolic hydroxy is replaced by a methoxy group, showed the lowest conversion value among the dimeric model compounds examined (Table 1). Neither the quinone **13** nor the conjugated aldehyde **15** were observed in the products. Uncharacterised polymerisation products were detected.

The apocynol **8**, in which the conjugated propenoidic chain of methyl (*E*)-ferulate ‡ **1** is replaced by an ethanolic chain (Scheme 4), showed the highest conversion value of all the

---

† The IUPAC name for coumaran is 2,3-dihydrobenzofuran.

‡ The IUPAC name for methyl ferulate is methyl 3-(4-hydroxy-3-methoxyphenyl)propenoate.

model compounds so far considered: even 30 min after the start of the reaction, the conversion value was 99%. The only isolated oxidation product was quinone **13** with a yield of 50 ± 3% 30 minutes after the start of the reaction. Also in this case further oxidation products obtained from the aromatic ring opening were not characterised and no polymerisation products were observed.

EPR investigation

The paramagnetic species active in the oxidation reactions of methyl (*E*)-ferulate **1** and methyl (*E*)-4-hydroxycinnamate **2** with dioxygen have been studied previously.[17,18]

At the reaction temperature the resonances observed in the X-band EPR spectrum were attributed to a phenoxy cobalt radical, formulated as $[Co^{III}(salen)(RO^-)(RO^\bullet)]$ (RO^- is the anion of the phenol compound, $RO^\bullet$ is the corresponding phenoxyl radical). The spectrum consists of an isotropic line centred at $g_{iso} \cong 2.00$; it shows a well resolved hyperfine interaction with the ^{59}Co ($I = 7/2$) nucleus with $A_{iso} \cong 10$ G, depending on the phenol substrate. The low value of the hyperfine coupling constant suggests that the unpaired electron is mainly located on the phenoxyl ligand. In spite of the isotropic appearance of the experimental spectrum at 298 K, its simulation, based on the hypothesis that only a single phenoxyl radical is present, did not give satisfactory results in the reaction solution. A result that was more unexpected and difficult to understand was that the spectrum recorded at 123 K[18] shows apparently isotropic lines centred at $g \cong 2.00$ with a hyperfine splitting about twice that observed in the spectrum recorded at the reaction temperature ($A \cong 18$ G, depending on the substrate). This difference between the hyperfine splittings in liquid and in frozen solution has already been observed in the literature for the [Co(salen)] adducts of the semiquinone radical anion by Kessel *et al.*[25] However these authors did not seem to be surprised by the difference and avoided any significant comment about its origin.

In order to rationalise these results and aiming to understand how many species were active in the oxidation mechanism, we changed the experimental procedure in recording the X-band EPR spectra, compared with that used in our previous papers:[18] 20 minutes after the start of the reaction, an aliquot of the reaction solution was drawn out and degassed by repeated freezing and evacuating procedures to eliminate dissolved O_2 from the reaction solution, then the X-band spectrum was recorded at 298 K in an argon atmosphere. The spectrum of the radical associated with the parent substrate methyl (*E*)-ferulate **1** (Fig. 1, line a), showed an increased resolution of the resonance lines compared with that reported in previous papers[18] because of the absence of broadening due to the interaction of the cobalt radical with dioxygen dissolved in the reaction solution. Such a spectrum was reproduced in a simulation by the superimposition of two isotropic species, which we called species I and II, with very similar *g* tensor values, each split into eight resonances by hyperfine coupling (Fig 1, line a′ and Table 3).

The X-band spectra of the deoxygenated solutions of the substrates **2**–**4** and **6**–**8** recorded under the same conditions are very similar to the spectrum observed in the case of methyl (*E*)-ferulate **1** and each of them was fitted with spin Hamiltonian parameter values attributable to two slightly different phenoxy cobalt radicals. For all the substrates, the cobalt radical species with the lower hyperfine coupling constant was called I, the other one was named II. The amount of species II is always comparable or lower than that of species I. Table 3 summarises the *g* tensor values which fit the X-band EPR spectra of phenoxy cobalt radicals at 298 K.

The reaction involving the β-*O*-4 type substrate **5**, in which the aromatic hydroxy is replaced by a methoxy group, did not form the phenoxy cobalt radicals.

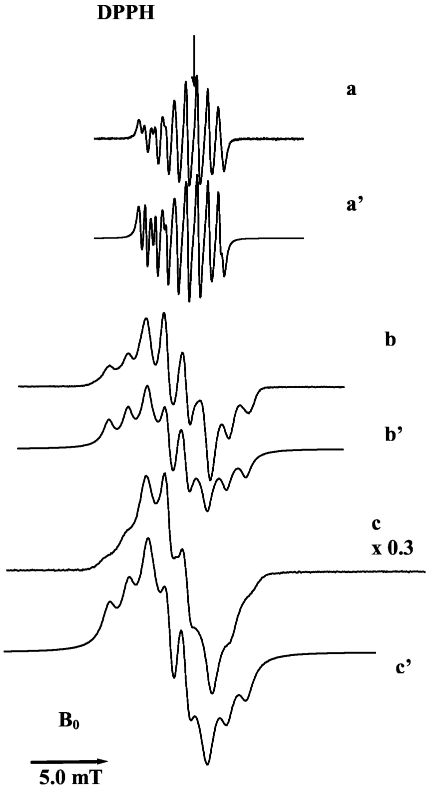

Fig. 1 X-Band EPR spectra of a chloroform solution of [Co(salen)] (6×10^{-3} M) and methyl (*E*)-ferulate (6×10^{-2} M) after 20 min exposure to O_2 at 1 MPa pressure, recorded at 298 K (line a, experimental; line a', simulated), at 123 K (line b, experimental; line b', simulated) and at 10 K (line c, experimental; line c', simulated).

The *A*-tensor values for both radical species derived from methyl (*E*)-ferulate **1** and the substrates which have a methoxy group as substituent *ortho* to the phenolic group, called "methoxyphenyl compounds" (the β-*O*-4 type compound **3**, the β-5 dimeric compound **6** and the monomeric substrate **8**), are higher than those for methyl (*E*)-4-hydroxycinnamate **2** and the substrates without any substituent *ortho* to the phenolic group, called "phenyl compounds" (the β-*O*-4 type substrate **4** and the β-5 type compound **7**). This result is in agreement with the differing tendencies of the various phenol ligands to accept electrons from cobalt, based on the redox potential of the free ligand molecules.[26,27]

The spectra of the sample aliquots taken 20 minutes after the start of the reaction of substrates **1**–**4** and **6**–**8** were recorded at 9.5 GHz upon cooling from 293 to 10 K. Above 200 K the resonance lines did not vary from those of the two phenoxy cobalt radicals observed at the reaction temperature (298 K) (Fig. 1, line a). Below this temperature, at 190 K, the lines underwent a rapid and dramatic change: they showed the shape previously reported for the radicals in a frozen solution at 123 K[18] (Fig. 1, line b). This effect may be attributed to a rapid change from the fast motion regime of the whole complex to a rigid regime in frozen chloroform solution. By cooling from 123 to 10 K the lines broadened and increased in intensity (Fig. 1, line c); the increase in the line width prevented distinction of the two phenoxy cobalt radicals detected at 298 K.

In order to improve the interpretation of the X-band spectrum, the change in the paramagnetic centres with temperature was followed from 200 K to 10 K using high frequency (HF) 190 GHz EPR spectra. The lifetime and the intensity of the X-band EPR spectra were considered for each of the phenoxy cobalt radicals produced in the investigated reactions. In the case of the HF-EPR experiments, because of the relatively high costs of the technique compared to conventional EPR spectroscopy, and the fact that the experiments are generally time

Table 4 X-Band EPR data which fit the spectra recorded at 123 K after 20 minutes of reaction on substrates reported in Schemes 1–4

Compound	*g*	A_{iso}/G[a]	$A_{//}$/G	$A_{\perp}$/G	$\Delta H_{//}$/G	$\Delta H_{\perp}$/G
1	2.002	9.6	18.7	5	6.8	12.0
2	1.999	8.6	16.9	4	6.1	16.8
3	2.000	9.4	19.3	4	5.8	18.3
4	2.000	8.2	16.7	4	4.5	16.7
6	2.000	9.1	19.3	4	6.9	18.5
7	2.000	8.7	17.2	4	6.3	16.7
8	2.001	10.1	20.0	5	6.6	13.8

[a] Calculated value.

consuming, the investigation was limited to a study of the phenoxy cobalt radicals produced from methyl (*E*)-ferulate **1**.

The 190 GHz EPR spectra of phenoxy cobalt radicals from methyl (*E*)-ferulate **1** showed at all temperatures from 200 to 10 K the typical frozen solution spectrum of an axially symmetric species ($g_{\perp}$ = 2.005 $g_{\parallel}$ = 1.995), with an increasing amplitude as the temperature is lowered (Fig. 2). The cobalt hyperfine splitting was presumably hidden by *g* strain effects; a second paramagnetic species was undetectable in the HF spectra. The *g* tensor anisotropy did not vary on lowering the temperature; this ruled out any hypothesis concerning the motion[28] of the complex.

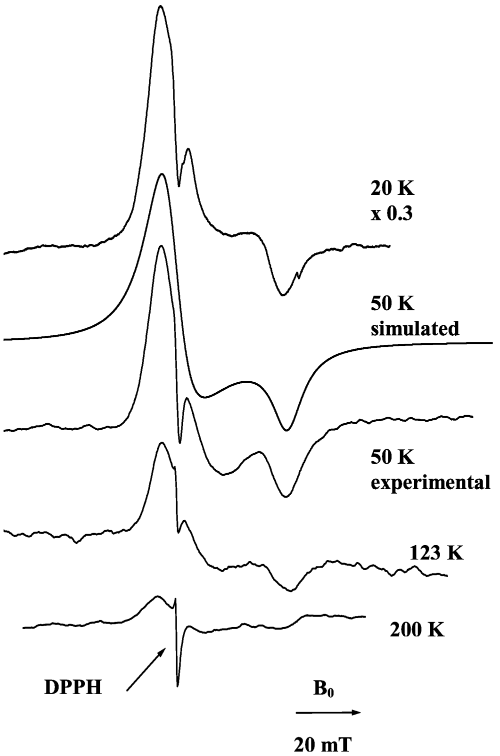

Fig. 2 HF-EPR spectra at 190 GHz of a chloroform solution of [Co(salen)] (6 × 10^{-3} M) and methyl (*E*)-ferulate (6 × 10^{-2} M) after 20 min exposure to O_2 at 1 MPa pressure, recorded at the indicated temperatures. Simulation of the spectrum recorded at 50 K is also given.

The X-band resonance lines for all the reacted substrate compounds were reproduced by the magnetic tensor values reported in Table 4, using substantially isotropic *g* tensor values, but axially anisotropic *A* tensor values. The experimental spectra were simulated using values of $A_{\parallel}$ and $A_{\perp}$ that reproduced the experimental A_{iso} value of species I better than for species II. Thus we suggest that species I largely prevails in frozen solution. The presence of small amounts of species II could tentatively be the reason for the unsatisfactory accuracy of the simulation (Fig. 1, lines b′ and c′). A similar poor accuracy was obtained in reproducing the HF 190 GHz resonance lines at 50 K (Fig. 2).

Combining the results of the high frequency measurements with those of the X-band, obtained at the same temperature, the cobalt phenoxy radical derived from methyl (*E*)-ferulate **1** displayed a large axial symmetry in the hyperfine coupling with the cobalt nucleus, but the *g* tensor components revealed significant anisotropy only at 190 GHz. It seems to us that the cobalt radical undergoes some rearrangement, which is frozen in the fast time scale of the 190 GHz spectra, but is averaged in the slower time scale of the X-band spectra. Similar behaviour can be attributed to all the cobalt radicals reported in this paper.

The reactions of all the substrates with dioxygen (1 MPa) reported in Schemes 1–4, carried out in chloroform in the presence of [Co(salen)], were monitored by X-band EPR spectroscopy, recording the spectra at 123 K of aliquots of the reaction solutions taken at different reaction times and immediately cooled in liquid nitrogen (see Experimental section). The trends in the signal intensity due to the phenoxy cobalt radicals *vs.* time at this temperature, calculated from the X-band spectra at 123 K for the methoxyphenyl compounds **1**, **3**, **6** and **8**, are shown in Fig. 3. The line intensity was evaluated by double integration of the resonance line areas and was comprehensive for both species I and II. Specifically: for the β-*O*-4 type compound **3** (line 3), at the reaction onset, the amount of paramagnetic species was about three times that obtained with methyl (*E*)-ferulate (line 1), but the intensity rapidly decreased and, after 30 minutes, it was almost the same as for methyl (*E*)-ferulate. This result suggests that the phenoxy cobalt radicals of a β-*O*-4 type substrate form more easily, but have a shorter lifetime than radicals of the monomeric substrate with the same substituents *ortho* to the aromatic hydroxy group.

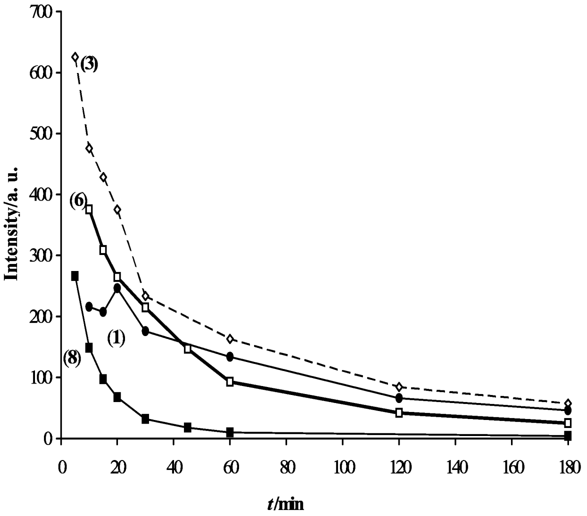

Fig. 3 Trends in intensity (arbitrary units) of the phenoxy cobalt radical signals *vs.* time (minutes) at the X-band, in chloroform solutions at 123 K, in the presence of [Co(salen)] (6 × 10^{-3} M) and the following substrates (6 × 10^{-2} M): methyl (*E*)-ferulate **1**, 3-(4-hydroxy-3-methoxyphenyl)-2-(2-methoxyphenoxy)propane-1,3-diol **3**, methyl (*E*)-[(2*RS*,3*SR*)-2,3-dihydro-2-(4-hydroxy-3-methoxyphenyl)-7-methoxy-3-methoxycarbonyl-1-benzofuran-5-yl] propenoate **6** and 1-(4-hydroxy-3-methoxyphenyl)ethanol **8**.

The β-5 dimeric compound **6** showed a signal attributed to the superoxocobalt derivative [Co^{III}(salen)(ROH)(O_2^-)] after 5 minutes of reaction. After 10 minutes, the signals of the phenoxy cobalt radicals became dominant; at the beginning they were about twice as high as the signals obtained with methyl (*E*)-ferulate **1**, then they rapidly decreased (line 6).

As has already been observed in the case of the β-*O*-4 type substrate **3**, this result suggests that also in the case of a β-5 type substrate the formation of phenoxy cobalt radicals is promoted, but such radicals have a shorter lifetime than the radicals formed by the corresponding monomeric derivative.

Monomeric compound **8** differs from the previously examined[18] monomeric substrates, **1** and **2**, because it has an α-hydroxyethane group in place of the propenoidic chain. Therefore, its behaviour should provide information on the role of the aliphatic hydroxys in the β-*O*-4 type substrates in the oxidation mechanism. Five minutes after the beginning of the reaction, the phenoxy radical signals had a considerable intensity, which then rapidly decreased to very small amplitudes. This result suggests that monomeric compounds with an α-hydroxyethane group form radicals having a shorter lifetime than the monomeric derivatives with a propenoidic chain and, from this point of view, are very similar to the dimeric derivatives with the same substituents *ortho* to the phenoxy group.

Fig. 4 reports the signal intensities of the phenoxy cobalt radicals formed from the phenyl compounds **2**, **4** and **7**. The intensities of such resonances are much lower than those of the corresponding methoxyphenyl compounds. Methyl (*E*)-4-hydroxycinnamate **2** displayed a spectrum the signals of which could be attributed to the phenoxy cobalt radical at each point in the reaction that was analysed; however the intensity was very low in the first 45 minutes of the reaction (line 2). For the β-*O*-4 type substrate **4**, after 5 minutes exposure to dioxygen, a very low intensity signal attributed to a superoxocobalt complex[18] was superimposed on the signals of the phenoxy cobalt radicals. After 20 minutes, only the signals of the latter species were present; their intensities were constant and low at each point in the reaction that was analysed (line 4). Nevertheless, as it was in the case of the methoxyphenyl compounds, the amount of phenoxy cobalt radicals of the dimeric substrate was higher but less persistent, compared with the corresponding monomeric substrate (line 2). In the case of the β-5 type dimeric compound **7**, the signals of the phenoxy cobalt radicals were observed at each reaction time; the intensities of such radicals were initially slightly higher than monomeric compound **2** (line 7).

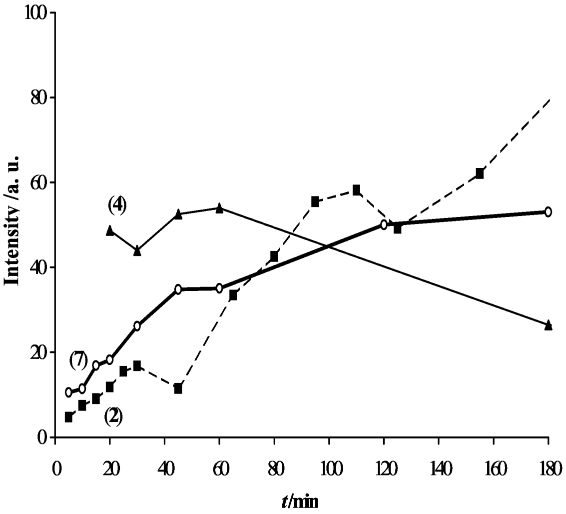

Fig. 4 Trends of intensity (arbitrary units) of the phenoxy cobalt radical signals *vs.* time (minutes) at the X-band, in chloroform solutions at 123 K, in the presence of [Co(salen)] (6×10^{-3} M) and the following substrates (6×10^{-2} M): methyl (*E*)-4-hydroxycinnamate **2**, 3-(4-hydroxyphenyl)-2-(2-methoxyphenoxy)propane-1,3-diol **4** and methyl (*E*)-[(2*RS*-3*SR*)-2,3-dihydro-2-(4-hydroxyphenyl)-3-methoxycarbonyl-1-benzofuran-5-yl]propenoate **7**.

Discussion and conclusions

The results of the previous investigations into the oxidation of propenoidic phenols[17,18] allowed the suggestion that their degradation occurs by the following three steps:

$$[\mathrm{Co^{II}(salen)}] + \mathrm{ROH} + \mathrm{O_2} \rightleftharpoons [\mathrm{Co^{III}(salen)(ROH)(O_2{}^-)}] \quad (1)$$

$$[\mathrm{Co^{III}(salen)(ROH)(O_2{}^-)}] + \mathrm{ROH} \rightleftharpoons [\mathrm{Co^{III}(salen)(ROH)(RO^{\bullet})}] + \mathrm{HO_2{}^-} \quad (2)$$

$$[\mathrm{Co^{III}(salen)(ROH)(RO^{\bullet})}] + \mathrm{HO_2{}^-} \rightleftharpoons [\mathrm{Co^{III}(salen)(RO^-)(RO^{\bullet})}] + \mathrm{H_2O_2} \quad (3)$$

Specifically:

1) The formation of the superoxocobalt derivative (reaction 1), in which the electron transfer from Co(II) to O_2 is promoted by the electron donor efficiency of the ROH ligand, *e.g.* substrate **1** > substrate **2**.[18]

2) Further reduction of $O_2{}^-$ to $HO_2{}^-$ together with the cobalt coordination of a second ROH molecule as RO• (reaction 2). The stability of [Co^{III}(salen)(ROH)(RO•)] is consistent with the trend in the reduction potentials of ROH: substrate **1** < substrate **2**.[26,27]

3) A third reaction step, only hypothesised, in which one ROH ligand loses H^+.

All the reactions are expected to be temperature dependent equilibria. For this reason, in the present paper the interaction with oxygen was studied both at 298 K and in frozen solution. In particular, the phenoxy cobalt radical produced by reaction (2) was studied by lowering the temperature from 298 K to 10 K 20 min after the start of the oxidation reaction. It was observed that:

i) for all substrates the simulation of the spectra at 298 K indicates the presence of two cobalt radical species (Table 3), very similar in their *g* tensor values, with species I having a lower hyperfine coupling with the cobalt nucleus than species II;

ii) species I and II, associated with both monomeric and dimeric methoxyphenyl compounds (**1**, **3**, **6** and **8**), showed higher values for the cobalt hyperfine coupling constants than for the phenyl compounds (**2**, **4** and **7**) (Table 3). This agrees with the lower one electron reduction potential of methoxyphenyl compounds;[26]

iii) in frozen solution species I became the major component. This species has a significant axial magnetic anisotropy of *g* and *A* tensor components, with $g_\perp > g_\parallel$ and $A_\parallel > A_\perp$. The X-band spectra simulation showed that the differences between the parallel and the perpendicular components of the hyperfine coupling constants are impressive in all paramagnetic species, thus we suggest that the high value of $A_\parallel$ is responsible for the double width of the X-band spectrum in frozen solution compared with the spectrum in fluid solution;

iv) as in frozen solutions species I was predominant and we tentatively assign this radical species to the protonated one in reaction (3). The proton was dissociated by increasing the temperature to 298 K;

v) as for the averaging of *g* tensor components in the slower time scale of X-band spectra, it seems to us very difficult to attribute the responsibility of this behaviour to some specific molecular or intramolecular motion[29] due to the persistence of the effect at very low temperatures. However, in the absence of data about the molecular structure of the phenoxy cobalt radicals, it seems to us hazardous to attribute the origin of the *g* average in the slower time scale.

The EPR monitoring of the phenoxy cobalt radicals for the methoxyphenyl compounds **1**, **3**, **6** and **8** (Fig. 3) showed that phenylpropanoids **3**, **6** and **8** generally produced higher amounts of radical than the phenylpropenoid **1**, at the start of the reaction, but such radicals disappeared more rapidly. We suggest that the electron donor effects, which were demonstrated[18] to promote reaction steps (1) and (2), are more efficient in propanoidic compounds **3**, **6** and **8** than in the propenoidic compound **1**, due to the absence of the conjugated side-chains.

A greater amount of radicals was also observed in the reactions of phenyl compounds **4** and **7** compared to **2**; however the very small amount of radicals derived from compounds **4** and **7** due to the lower basic character of the phenyl compounds, shows the absence of conjugation with the side-chain to be less significant.

A comparison between the trends in the intensities of the phenoxy cobalt radicals *vs.* reaction time (Fig. 3 and 4) and the conversion rates (Table 1), demonstrates that:

i) the higher conversion rates at 30 min from the onset of the oxidation of the propanoidic phenols **3**, **6** and **8** with respect to the propenoidic phenol **1** correspond to a faster decrease in the amounts of radicals associated with propanoidic phenols;

ii) the lower conversion rates of phenyl compounds **2**, **4** and **7** with respect to methoxyphenyl compounds **1**, **3**, **6** and **8**, agrees with the longer lifetime of the radicals associated with phenyl compounds.

The results of both conversion data and spectroscopic investigations afford the suggestion that the lifetime of the phenoxy radicals is related to the conversion rates of the substrates. Different reaction pathways not involving the formation of phenoxy radicals lead to different products and cannot be considered as a comparison.

Acknowledgements

This research has been supported by the Italian Institute for Science and Technology of Materials (INSTM).

References

1 H. Wariishi, K. Valli and M. H. Gold, *Biochemistry*, 1989, **28**, 6017–6023.
2 J. S. Dordick, M. A. Marletta and A. M. Klibanov, *Proc. Natl. Acad. Sci. USA*, 1986, **83**, 6255.
3 H. Hammel, B. Kalyanaraman and T. Kent Kirk, *Proc. Natl. Acad. Sci. USA*, 1986, **83**, 3707.
4 G. A. Swan, *Fortschr. Chem. Org. Naturst.*, 1974, **31**, 521.
5 T. Higuchi, *Biosynthesis and biodegradation of wood components*, Academic Press, New York, 1985.
6 H. Wariishi, K. Valli and M. Gold, *Biochemistry*, 1989, **28**, 6017.
7 H. L. Chum and M. M. Baaizer, *The electrochemisty of Biomass and Derived Material*, ACS Monograph, Washington, 1985.
8 J. Janson and T. Fullerton, *Holzforschung*, 1987, **41(6)**, 359.
9 F. Bertaud, J. P. Crouè and B. Legube, *Ozone: Sci. Eng.*, 2001, **23**, 139.
10 V. L. Pardini, R. R. Vargas, H. Viertler and J. H. P. Utley, *Tetrahedron*, 1992, **48**, 7221.
11 C. Crestini and D. S. Argyropoulos, *Bioorg. Med. Chem.*, 1998, **6**, 2161.
12 R. Patt, H. J. Mielisch, O. Kordsachia and N. L. Schubert, *Proceedings of International Pulp Bleaching Conference*, Gummerus Kirjapaino Oy, Jyväskylä, Helsinki, Finland, 1998, p. 111.
13 R. S. Drago, B. B. Corden and C. W. Barnes, *J. Am. Chem. Soc.*, 1986, **108**, 2453.
14 J. J. Bozell, B. R. Hames and D. R. Dimmel, *J. Org. Chem.*, 1995, **60**, 2398.
15 T. Elder and J. J. Bozell, *Holzforschung*, 1996, **50**, 24–30.
16 A. Haikarainen, K. Kervinen, J. Sipila, T. Repo, G. Brunow and M. Leskala, *Proceedings of International Symposium on Wood and Pulping Chemistry*, Nice, France, 2001, p. 231.
17 E. Bolzacchini, A. M. Brambilla, M. Orlandi and B. Rindone, *Life Chem. Rep.*, 1995, **13**, 71; A. Bassoli, A. M. Brambilla, E. Bolzacchini, F. Chioccara, F. Morazzoni, M. Orlandi and B. Rindone, *ACS Symp. Ser.*, 1996, **626**, 92.
18 E. Bolzacchini, L. Bocchio Chiavetto, C. Canevali, F. Morazzoni, M. Orlandi and B. Rindone, *J. Mol. Catal. A: Chem.*, 1996, **112**, 347; E. Bolzacchini, C. Canevali, F. Morazzoni, M. Orlandi, B. Rindone and R. Scotti, *J. Chem. Soc., Dalton Trans.*, 1997, 4695.
19 J. Sipila, C. Wiik, K. Koli, P. Karhunen, S. L. Maunu and T. Liitia, *Proceedings of International Symposium on Wood and Pulping Chemistry*, Nice, France, 2001, pp. 9–12.
20 C. W. Bailey and C. W. Dence, *Tappi J.*, 1969, **59**(3), 491.
21 J. Sipila and K. Syrjanen, *Holzforschung*, 1995, **49**, 325.
22 M. Orlandi, B. Rindone, G. Molteni, P. Rummakko and G. Brunow, *Tetrahedron*, 2001, **57**(2), 371.
23 A. K. Hassan, L. A. Pardi, J. Krzystek, A. Sienkiewicz, P. Goy, M. Rohrer and L. C. Brunel, *J. Magn. Reson.*, 2000, **142**, 300–312.
24 J. Gierer, F. Imsgard and I. Noren, *Acta Chem. Scand., Ser. B*, 1977, 561.
25 S. L. Kessel, R. M. Emberson, P. G. Debrunner and D. N. Hendrickson, *Inorg. Chem.*, 1980, **19**, 1170.
26 S. V. Jovanovic, M. Tosic and M. G. Simic, *J. Phys. Chem.*, 1991, **95**, 10824.
27 J. Lind, X. Shen, T. E. Eriksen and G. Merényi, *J. Am. Chem. Soc.*, 1990, **112**, 479.
28 S. Van Doorslaer and A. Schweiger, *J. Phys. Chem. B*, 2000, **104**, 2919.
29 Z. Liang and J. Freed, *J. Phys. Chem. B*, 1999, **103**, 6384.